

Parameterized Projected Bellman Operator

Theo Vincent^{1,2,*} Alberto Maria Metelli³ Boris Belousov¹
Jan Peters^{1,2,4,5} Marcello Restelli³ Carlo D'Eramo^{2,4,6}

¹German Research Center for AI (DFKI) ²TU Darmstadt ³Politecnico di Milano
⁴Hessian.ai ⁵Centre for Cognitive Science ⁶CAIDAS, University of Würzburg

Abstract

Approximate value iteration (AVI) is a family of algorithms for reinforcement learning (RL) that aims to obtain an approximation of the optimal value function. Generally, AVI algorithms implement an iterated procedure where each step consists of (i) an application of the Bellman operator and (ii) a projection step into a considered function space. Notoriously, the Bellman operator leverages transition samples, which strongly determine its behavior, as uninformative samples can result in negligible updates or long detours, whose detrimental effects are further exacerbated by the computationally intensive projection step. To address these issues, we propose a novel alternative approach based on learning an approximate version of the Bellman operator rather than estimating it through samples as in AVI approaches. This way, we are able to (i) generalize across transition samples and (ii) avoid the computationally intensive projection step. For this reason, we call our novel operator *projected Bellman operator* (PBO). We formulate an optimization problem to learn PBO for generic sequential decision-making problems, and we theoretically analyze its properties in two representative classes of RL problems. Furthermore, we theoretically study our approach under the lens of AVI and devise algorithmic implementations to learn PBO in offline and online settings by leveraging neural network parameterizations. Finally, we empirically showcase the benefits of PBO w.r.t. the regular Bellman operator on several RL problems.

Introduction

Value-based reinforcement learning (RL) is a popular class of algorithms for solving sequential decision-making problems with unknown dynamics (Sutton and Barto 2018). For a given problem, value-based algorithms aim at obtaining the most accurate estimate of the expected return from each state, i.e., a value function. For instance, the well-known value-iteration algorithm computes value functions by iterated applications of the Bellman operator (Bellman 1966), of which the true value function is the fixed point. Although the Bellman operator can be applied in an exact way in dynamic programming, it is typically estimated from samples *at each application* when dealing with problems with unknown models, i.e., empirical Bellman operator (Watkins

1989; Bertsekas 2019). Intuitively, the dependence of the empirical version of value iteration on the samples has an impact on the efficiency of the algorithms and on the quality of the obtained estimated value function, which becomes accentuated when solving continuous problems that require function approximation, e.g., approximate value iteration (AVI) (Munos 2005; Munos and Szepesvári 2008). Moreover, in AVI approaches, costly function approximation steps are needed to project the output of the Bellman operator back to the considered value function space.

In this paper, we introduce the *projected Bellman operator* (PBO), which consists of a function $\Lambda : \Omega \rightarrow \Omega$ defined on the parameters $\omega \in \Omega$ of the value function approximator Q_ω . Contrary to the standard (empirical) Bellman operator Γ , which acts on the value functions Q_k to compute targets that are then projected to obtain Q_{k+1} , our PBO Λ acts on the parameters of the value function to directly compute updated parameters $\omega_{k+1} = \Lambda(\omega_k)$ (Figure 1). The advantages of our approach are twofold: (i) PBO is applicable for an arbitrary number of iterations without using further samples, and (ii) the output of PBO always belongs to the considered value function space as visualized in Figure 2, thus avoiding the costly projection step which is required when using the Bellman operator coupled with function approximation. We show how to estimate PBO from transition samples by leveraging a parametric approximation which we call *parameterized* PBO, and we devise two algorithms for offline and online RL to learn it. Starting from initial parameters ω_0 , AVI approaches obtain consecutive approximations of the value function Q_{ω_k} by applying the Bellman operator iteratively over samples (Figure 2b). Instead, we make use of the samples to learn the PBO only. Then, starting from initial parameters ω_0 , PBO can produce a chain of value function parameters of *arbitrary* length (as shown with the blue lines in Figure 2a) without requiring further samples. This means an

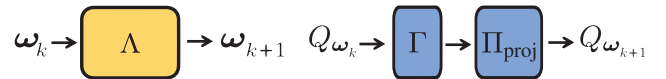


Figure 1: PBO Λ (left) operates on value function parameters as opposed to AVI (right), that uses the empirical Bellman operator Γ followed by the projection operator Π_{proj} .

*Correspondence to: theo.vincent@dfki.de

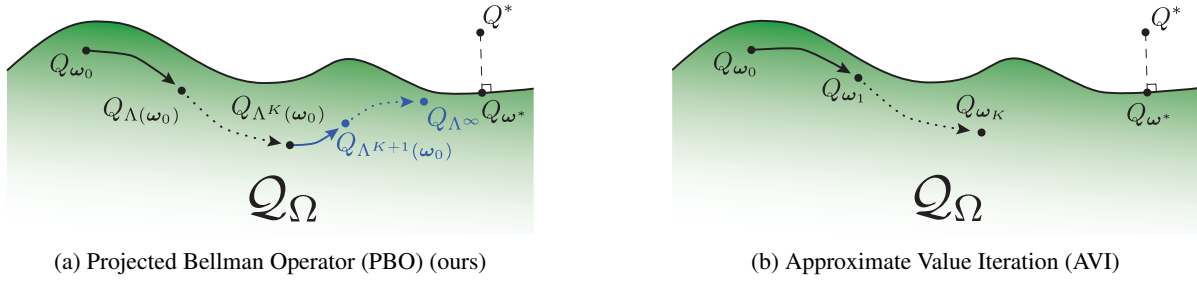


Figure 2: Behavior of our PBO and AVI in the parametric space of value functions \mathcal{Q} . Here Q^* , Q_{ω^*} , and Q_{Λ^∞} , are respectively the optimal value function, its projection on the parametric space, and the fixed point of PBO. Contrary to the regular Bellman operator, PBO can be applied for an arbitrary number of steps (blue lines) without requiring additional samples.

accurate approximation of PBO can compute optimal value function parameters starting from any initial parameters in the chosen space without requiring additional samples.

Related work

Several papers in the literature proposed variants of the standard Bellman operator to induce certain behaviors. We review these approaches, noting that they all act on the space of action-value functions, thus needing a costly projection step onto the considered function space. Conversely, to the best of our knowledge, our work is the first attempt to obtain an alternative Bellman operator that avoids the projection step by directly acting on the parameters of value functions.

Bellman operator variations. Variants of the Bellman operator are widely studied for entropy-regularized MDPs (Neu, Jonsson, and Gómez 2017; Geist, Scherrer, and Pietquin 2019; Belousov and Peters 2019). The *softmax* (Haarnoja et al. 2017; Song, Parr, and Carin 2019), *mellowmax* (Asadi and Littman 2017), and *optimistic* (Tosatto et al. 2019) operators are all examples of variants of the Bellman operator to obtain maximum-entropy exploratory policies. Besides favoring exploration, other approaches address the limitations of the standard Bellman operator. For instance, the *consistent* Bellman operator (Bellemare et al. 2016) is a modified operator that addresses the problem of inconsistency of the optimal action-value functions for sub-optimal actions. The *distributional* Bellman operator (Bellemare, Dabney, and Munos 2017) enables operating on the whole return distribution instead of its expectation, i.e., the value function (Bellemare, Dabney, and Rowland 2023). Furthermore, the *logistic* Bellman operator uses a logistic loss to solve a convex linear programming problem to find optimal value functions (Bas-Serrano et al. 2021). Finally, the *Bayesian* Bellman operator is employed to infer a posterior over Bellman operators centered on the true one (Fellows, Hartikainen, and Whiteson 2021). Note that our PBO can be seamlessly applied to any of these variants of the standard Bellman operator. Finally, we recognize that learning an approximation of the Bellman operator shares some similarities with learning a reward-transition model in reinforcement learning. However, we point out that our approach is profoundly different, as we map action-value parameters to other action-value parameters, in contrast to model-based

reinforcement learning, which maps states and actions to rewards and next states.

Operator learning. Literature in operator learning is mostly focused on supervised learning, with methods for learning operators over vector spaces (Micchelli and Pontil 2005) and parametric approaches for learning non-linear operators (Chen and Chen 1995), with a resurgence of recent contributions in deep learning. For example, Kovachki et al. (2021, 2023) learn mappings between infinite function spaces with deep neural networks, or Kissas et al. (2022) apply an attention mechanism to learn correlations in the target function for efficient operator learning. We note that our work on the learning of the Bellman operator in reinforcement learning is orthogonal to methods for operator learning in supervised learning, and could potentially benefit from advanced techniques in the literature.

HyperNetworks. Our approach shares similarities with HyperNetworks (Ha, Dai, and Le 2016; Sarafian, Keynan, and Kraus 2021; Beck et al. 2023). In the classification proposed in Chauhan et al. (2023), PBO distinguishes itself by taking as input the parameters generated at the previous forward pass. In this sense, PBO can be seen as a recurrent variant of HyperNetworks that generates a series of parameters representing the consecutive Bellman iterations.

Preliminaries

We consider discounted Markov decision processes (MDPs) defined as $\mathcal{M} = \langle \mathcal{S}, \mathcal{A}, \mathcal{P}, \mathcal{R}, \gamma \rangle$, where \mathcal{S} is a measurable state space, \mathcal{A} is a finite, measurable action space, $\mathcal{P} : \mathcal{S} \times \mathcal{A} \rightarrow \Delta(\mathcal{S})^1$ is the transition kernel of the dynamics of the system, $\mathcal{R} : \mathcal{S} \times \mathcal{A} \rightarrow \mathbb{R}$ is a reward function, and $\gamma \in [0, 1]$ is a discount factor (Puterman 1990). A policy $\pi : \mathcal{S} \rightarrow \mathcal{A}$ is a function mapping a state to an action, inducing a value function $V^\pi(s) \triangleq \mathbb{E} \left[\sum_{t=0}^{+\infty} \gamma^t \mathcal{R}(S_t, \pi(S_t)) | S_0 = s \right]$ representing the expected cumulative discounted reward starting in state s and following policy π thereafter. Similarly, the action-value function $Q^\pi(s, a) \triangleq \mathbb{E} \left[\sum_{t=0}^{+\infty} \gamma^t \mathcal{R}(S_t, A_t) | S_0 = s, A_0 = a, A_t = \pi(S_t) \right]$ is the expected discounted cumulative reward executing action a in state s , following policy π thereafter. RL aims to find

¹ $\Delta(\mathcal{X})$ denotes the set of probability measures over the set \mathcal{X} .

an optimal policy π^* yielding the optimal value function $V^*(s) \triangleq \max_{\pi: \mathcal{S} \rightarrow \mathcal{A}} V^\pi(s)$ for every $s \in \mathcal{S}$ (Puterman 1990). The (optimal) Bellman operator Γ^* is a fundamental tool in RL for obtaining optimal policies, defined as:

$$(\Gamma^*Q)(s, a) \triangleq \mathcal{R}(s, a) + \gamma \int_{\mathcal{S}} \mathcal{P}(\text{ds}'|s, a) \max_{a' \in \mathcal{A}} Q(s', a'), \quad (1)$$

for all $(s, a) \in \mathcal{S} \times \mathcal{A}$. It is well-known that Bellman operators are γ -contraction mappings in L_∞ -norm, such that their iterative application leads to the unique fixed point $\Gamma^*Q^* = Q^*$ in the limit (Bertsekas 2015). We consider using function approximation to represent value functions and denote Ω as the space of their parameters. Thus, we define $\mathcal{Q}_\Omega = \{Q_\omega : \mathcal{S} \times \mathcal{A} \rightarrow \mathbb{R} | \omega \in \Omega\}$ as the set of value functions representable by parameters of Ω .

Projected Bellman operator

The application of the Bellman operator in RL requires transition samples (Equation 1) and a costly projection step onto the used function space (Munos 2003, 2005; Munos and Szepesvári 2008). We are interested in obtaining an operator that overcomes these issues while emulating the behavior of the regular Bellman operator. Hence, we introduce the *projected Bellman operator* (PBO), which we define as follows.

Definition 1. Let $\mathcal{Q}_\Omega = \{Q_\omega : \mathcal{S} \times \mathcal{A} \rightarrow \mathbb{R} | \omega \in \Omega\}$ be a function approximation space for the action-value function, induced by the parameter space Ω . A projected Bellman operator (PBO) is a function $\Lambda : \Omega \rightarrow \Omega$, such that

$$\Lambda \in \arg \min_{\Lambda: \Omega \rightarrow \Omega} \mathbb{E}_{(s,a) \sim \rho, \omega \sim \nu} (\Gamma^*Q_\omega(s, a) - Q_{\Lambda(\omega)}(s, a))^2, \quad (2)$$

for state-action and parameter distributions ρ and ν .

Note that Γ^* is the regular optimal Bellman operator on \mathcal{Q}_Ω . Conversely, PBO is an operator Λ acting on action-value function parameters $\omega \in \Omega$. In other words, this definition states that a PBO is the mapping $\Omega \rightarrow \Omega$ that most closely emulates the behavior of the regular optimal Bellman operator Γ^* . Thus, by acting on the parameters ω of action-value functions Q_ω , PBO can be applied for an arbitrary number of steps starting from any initial parameterizations ω_0 , without using additional transition samples. Moreover, being a mapping between parameters ω_k to parameters ω_{k+1} , PBO does not require the costly projection step needed by the regular Bellman operator.

Learning projected Bellman operators

The PBO is unknown and has to be estimated from samples. We propose to approximate PBO with a *parameterized PBO* Λ_ϕ differentiable w.r.t. its parameters $\phi \in \Phi$, enabling the use of gradient descent on a loss function.² We do so by formulating an empirical version of the problem (2) that can be optimized via gradient descent by using a given dataset of parameters $\omega \in \mathcal{W}$ and transitions $(s, a, r, s') \in \mathcal{D} \sim \rho$. Crucially, we can leverage PBO to augment the dataset of

²For ease of presentation, we use PBO and parameterized PBO interchangeably whenever clear from the context.

Algorithm 1: Projected FQI & Projected DQN

- 1: **Inputs:**
 - samples $\mathcal{D} = \{\langle s_j, a_j, r_j, s'_j \rangle\}_{j=1}^J$;
 - parameters $\mathcal{W} = \{\omega_l\}_{l=1}^L$;
 - #Bellman iterations K ;
 - initial parameters ϕ of parameterized PBO Λ_ϕ ;
 - #Epochs E .
 - 2: **for** $e \in \{1, \dots, E\}$ **do**
 - 3: $\bar{\phi} = \phi$
 - 4: **for** some training steps **do**
 - 5: Collect samples \mathcal{D}' with policy given by $Q_{\Lambda_\phi^K(\omega)}$
 - 6: $\mathcal{D} \leftarrow \mathcal{D} \cup \mathcal{D}'$
 - 7: Gradient descent over parameters ϕ minimizing loss (3) or (4) using \mathcal{D} or a batch of \mathcal{D} and \mathcal{W} .
 - 8: **end for**
 - 9: **end for**
 - 10: **Return:** Parameters ϕ of parameterized PBO Λ_ϕ
-

parameters $\omega \in \mathcal{W}$ with sequences generated by PBO at no cost of additional samples. The resulting loss is

$$\mathcal{L}_{\Lambda_\phi} = \sum_{k=1}^K \sum_{\substack{(s,a) \in \mathcal{D} \\ \omega \in \mathcal{W}}} \left(\Gamma Q_{\Lambda_\phi^{k-1}(\omega)}(s, a) - Q_{\Lambda_\phi^k(\omega)}(s, a) \right)^2, \quad (3)$$

where K is an arbitrary number of optimal Bellman operator iterations. Note that for $K = 1$ we obtain the empirical version of the optimization problem (2). An additional idea is to add a term that corresponds to an infinite number of iterations, i.e., the fixed point,

$$\mathcal{L}_{\Lambda_\phi^\infty} = \mathcal{L}_{\Lambda_\phi} + \underbrace{\sum_{(s,a) \in \mathcal{D}} \left(\Gamma Q_{\Lambda_\phi^\infty}(s, a) - Q_{\Lambda_\phi^\infty}(s, a) \right)^2}_{\text{Fixed point term}}, \quad (4)$$

where Λ_ϕ^∞ is the fixed point of the parameterized PBO. Note that the addition of the fixed-point term is only possible for classes of parameterized PBOs where the fixed point can be computed, and the result is differentiable w.r.t. the parameters ϕ , as we describe in the following section.

We can now devise two algorithms to learn PBO in both offline and online RL. Our algorithms can be seen as variants of the offline algorithm fitted Q -iteration (FQI) (Ernst, Geurts, and Wehenkel 2005) and online algorithm deep Q -network (DQN) (Mnih et al. 2015); thus, we call them *projected fitted Q -iteration* (ProFQI) and *projected deep Q -network* (ProDQN).

Algorithm 1 compactly describes both ProFQI and ProDQN, highlighting the additional steps required for the online setting (i.e., ProDQN). Both ProFQI and ProDQN are given initial randomly sampled datasets of transitions and parameters of PBO. As an online algorithm, ProDQN periodically adds new transitions to the dataset by executing a policy derived from the action-value function obtained by applying the current approximation of PBO for K times. For stability reasons, we perform gradient descent steps only on the parameters ϕ of $Q_{\Lambda_\phi^K}$ in the loss

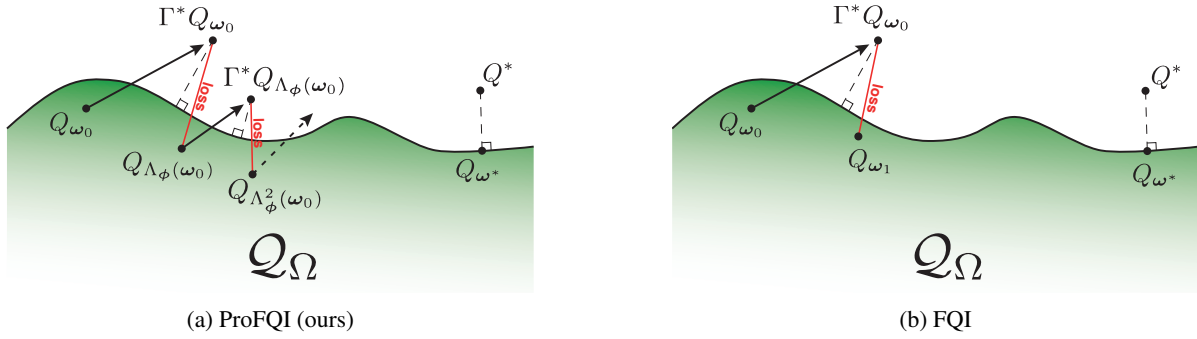


Figure 3: Behavior of ProFQI and FQI in the function space \mathcal{Q}_Ω for one iteration. The ability to apply PBO for an arbitrary number of times enables ProFQI to generate a sequence of action-value functions $Q_{\Lambda_\phi^k}(\omega_0)$ that can be used to enrich the loss function to learn PBO (see red lines). On the contrary, one iteration of FQI corresponds to a single application of the Bellman operator followed by the projection step onto the function space.

(Equation 3), excluding the ones corresponding to the target $\Gamma Q_{\Lambda_\phi^{k-1}}$, as commonly done in semi-gradient methods (Sutton and Barto 2018). Similar to Mnih et al. (2015), the target parameters are updated periodically after an arbitrary number of iterations. Soft updates, e.g., Polyak averaging (Lillicrap et al. 2015), can also be used. As also illustrated by Figure 3, ProFQI and FQI behave substantially differently in the space of action-value functions \mathcal{Q}_Ω . ProFQI aims to learn PBO to subsequently use it to generate a sequence $(Q_{\omega_0}, Q_{\Lambda_\phi(\omega_0)}, Q_{\Lambda_\phi^2(\omega_0)}, \dots)$ of action-value parameters starting from any parameters ω_0 ; on the contrary, FQI generates a sequence of action-value functions $(Q_{\omega_0}, Q_{\omega_1}, \dots)$ that need to be projected onto the function space at every iteration. Moreover, ProFQI can apply PBO multiple times to form a richer loss than the one for FQI, which can only consider one application of the Bellman operator at a time (see red lines in Figure 3a and 3b).

Analysis of projected Bellman operator

Besides the practical advantages of being independent of samples and not needing a projection step, PBO plays an interesting role when investigated theoretically in the AVI framework. In particular, the ability of PBO to iterate for an arbitrary number of times enables us to theoretically prove its benefit in terms of approximation error at a given timestep K by leveraging the following established results in AVI.

Theorem 2. (See Theorem 3.4 of Farahmand (2011)) Let $K \in \mathbb{N}^*$, ρ, ν two distribution probabilities over $\mathcal{S} \times \mathcal{A}$. For any sequence $(Q_k)_{k=0}^K \subset B(\mathcal{S} \times \mathcal{A}, R_\gamma)$ where R_γ depends on reward function and discount factor, we have

$$\|Q^* - Q^{\pi_K}\|_{1,\rho} \leq C_{K,\gamma,R_\gamma} \quad (5)$$

$$+ \inf_{r \in [0,1]} F(r; K, \rho, \gamma) \underbrace{\left(\sum_{k=1}^K \alpha_k^{2r} \|\Gamma^* Q_{k-1} - Q_k\|_{2,\nu}^2 \right)}_{\text{ProFQI}},$$

where α_k and C_{K,γ,R_γ} do not depend on the sequence $(Q_k)_{k=0}^K$. $F(r; K, \rho, \gamma)$ relies on the concentrability coefficients of the greedy policies w.r.t. the value functions.

This theorem shows that the distance between the value function and the optimal value function (left-hand side of Equation (5)) is upper-bounded by a quantity proportional to the approximation errors $\|\Gamma^* Q_{k-1} - Q_k\|_{2,\nu}^2$ at each iteration k . As highlighted in Equation (5), at every iteration k , the loss of FQI contains only one term of the sum. Conversely, the loss of ProFQI contains the entire sum of approximation errors from iteration $k = 1$ to K . This means that while FQI minimizes the approximation error for a single iteration at a time, ProFQI minimizes the approximation errors for multiple iterations, thus effectively reducing the upper bound on the approximation error at iteration K .

In the following, we empirically showcase this theoretical advantage and we further analyze the properties of PBO for two representative classes of RL problems, namely (i) finite MDPs and (ii) linear quadratic regulators (Bradtke 1992; Pang and Jiang 2021). Proofs of the following results and additional analysis of PBO in low-rank MDPs (Agarwal et al. 2020; Sekhari et al. 2021) can be found in the appendix.

Finite Markov decision processes

Let us consider finite state and action spaces of cardinality N and M , respectively, and a tabular setting with $\Omega = \mathbb{R}^{N \cdot M}$. Given the use of tabular approximation, it is intuitive that each entry of the table can be modeled with a different single parameter, i.e., there is a bijection between \mathcal{Q}_Ω and Ω , which allows us to write, for ease of notation, the parameters of the action-value function as Q instead of ω .

Proposition 3. The PBO exists, and it is equal to the optimal Bellman operator

$$\Lambda^*(Q) = R + \gamma P \max_{a \in \mathcal{A}} Q(\cdot, a). \quad (6)$$

Note that PBO for finite MDPs is a γ -contraction mapping for the L_∞ -norm, like an optimal Bellman operator. As an example of finite MDP, we consider the chain-walk environment in Figure 5, with a chain of length $N = 20$. We parameterize value functions as tables to leverage our theoretical results on finite MDPs. In Figure 4, we show the ℓ_2 -norm of the difference between the optimal action-value function and the action-value function computed with FQI

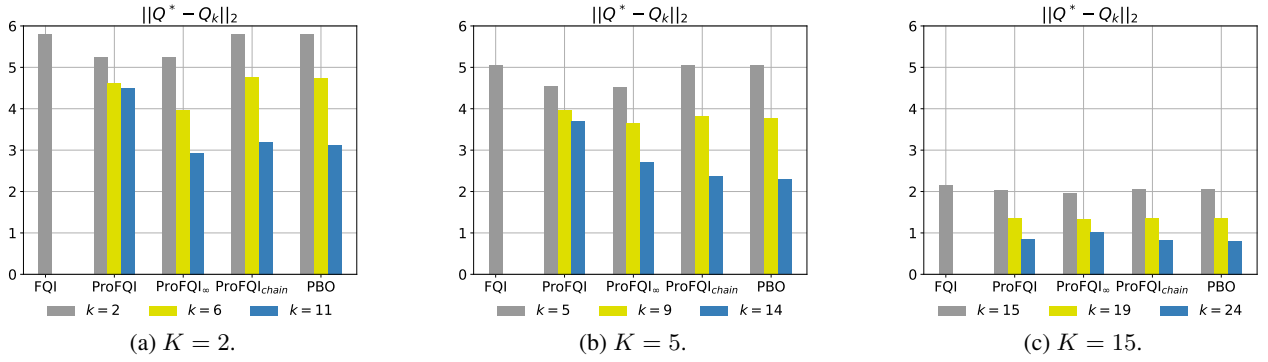


Figure 4: ℓ_2 -norm of the difference between the optimal action-value function and the approximated action-value function on chain-walk. Here K is the number of iterations included in the training loss (3) of PBO, while k is the number of PBO applications after training. Results are averaged over 20 seeds. Note that PBO enables using $k \geq K$ compared to FQI, which results in better convergence for increasing k for each fixed $K \in \{2, 5, 15\}$.

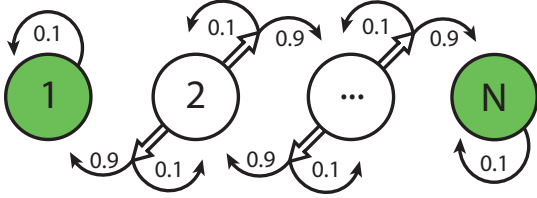


Figure 5: Test task: chain-walk from Munos (2003). The reward is 0 in all states except green states where it equals 1.

and ProFQI. We consider three different values of Bellman iterations, namely $K \in \{2, 5, 15\}$. For FQI, the K iterations are the regular iterations where the empirical Bellman operator is applied to the current approximation of the action-value function. For ProFQI, K is the number of iterations included in the PBO loss. This ensures a fair comparison, given that both methods have access to the same number of Bellman iterations. Once PBO is trained, we apply it for different numbers of iterations $k \geq K$, on given action-value function parameters. In Figure 4, ProFQI uses a linear approximation of PBO trained with the loss (3), ProFQI $_{\infty}$ uses a linear approximation of PBO trained with the loss (4), ProFQI $_{\text{chain}}$ uses the closed-form PBO in Equation (6) considering R and P as unknown parameters to learn, and PBO indicates the use of the same closed-form solution assuming known R and P . For the three variants of ProFQI, we observe that the approximation error decreases as the number of PBO iterations increases, evincing that PBO accurately emulates the true Bellman operator. In the case of $K = 2$ and $K = 5$, we see that ProFQI $_{\infty}$ and ProFQI $_{\text{chain}}$ obtain a better approximation of the action-value function compared to ProFQI, thanks to, respectively, the inclusion of fixed point in the loss and the use of the closed-form solution. Interestingly, in the case of $K = 15$, ProFQI $_{\infty}$ obtains a slightly worse approximation than ProFQI. We explain this behavior with the fact that when the linear approximation is inadequate for modeling PBO, adding the fixed point in the loss could harm the estimate.

Linear quadratic regulation

Now, we consider the continuous MDPs class of linear quadratic regulator (LQR) with $\mathcal{S} = \mathcal{A} = \mathbb{R}$. The transition model $\mathcal{P}(s, a) = As + Ba$ is deterministic and the reward function $\mathcal{R}(s, a) = Qs^2 + 2Ssa + Ra^2$ is quadratic, where A, B, Q, S and R , are constants inherent to the MDP. We choose to parameterize the action-value functions with a 2-dimensional parameter vector $\mathcal{Q}_{\Omega} = \{(s, a) \mapsto Gs^2 + 2Isa + Ma^2 | (G, I) \in \mathbb{R}^2\}$ where M is a chosen constant, for visualization purposes.

Proposition 4. *PBO exists, and for any $\omega \in \mathbb{R}^2$, its closed form is given by:*³

$$\Lambda^* : \omega = \begin{bmatrix} G \\ I \end{bmatrix} \mapsto \begin{bmatrix} Q + A^2(G - \frac{I^2}{M}) \\ S + AB(G - \frac{I^2}{M}) \end{bmatrix}. \quad (7)$$

We leverage our theoretical analysis for LQR (Bradtke 1992; Pang and Jiang 2021) by parameterizing value functions accordingly, and we conduct a similar analysis to the one for chain-walk. This time, we evaluate the distance between the optimal action-value function parameters, which can be computed analytically, and the estimated ones. We use the closed-form solution obtained in Equation 7 assuming the parameters (A, B, Q, S) known (PBO), and unknown (ProFQI $_{\text{LQR}}$). Figure 6 confirms the pattern observed on the chain-walk. ProFQI and ProFQI $_{\infty}$ obtain a better approximation than FQI, which is reasonably worse than ProFQI $_{\text{LQR}}$ and PBO. We also observe that ProFQI $_{\text{LQR}}$ obtains a significantly better approximation than the other variants for a large number of iterations (blue bars), confirming the advantages of exploiting the closed-form solution of PBO for finite MDPs. We additionally show the sequence of parameters corresponding to the iterations of FQI, ProFQI $_{\text{LQR}}$, and ProFQI, in Figure 7. The training is done with $K = 2$. The sequence starts from the chosen initial parameters $(G, I) = (0, 0)$ for all algorithms and proceeds towards the optimal parameters, which are computed analytically. Both ProFQI and ProFQI $_{\text{LQR}}$ apply the PBO learned

³Under a mild assumption over the sample distribution, see in the Proofs section in the appendix.

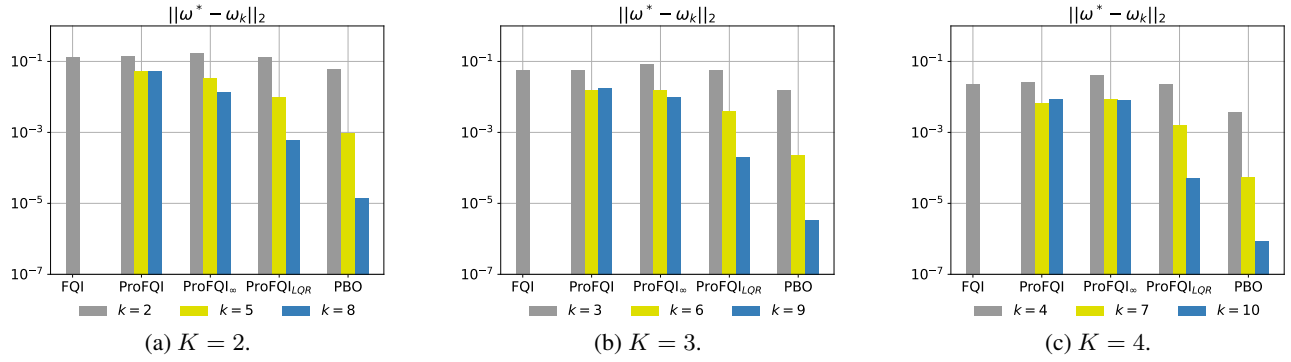


Figure 6: ℓ_2 -norm of the difference between the optimal action-value function parameters and the estimated ones on LQR. Here K is the number of iterations included in the training loss (3) of PBO, while k is the number of PBO applications after training. Results are averaged over 20 seeds. Similar to Figure 4, PBO shows improved convergence for $k \geq K$ compared to FQI.

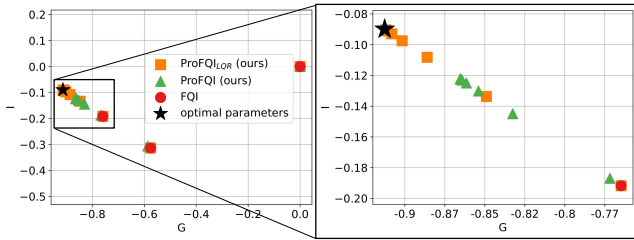


Figure 7: Behavior of FQI and ProFQI in the space of action-value function parameters (G, I) for LQR. FQI is performed with 2 iterations, and ProFQI uses a PBO trained with $K = 2$, for the sake of fair comparison. Notably, ProFQI can leverage PBO by applying it for 8 iterations, being able to get closer to the optimal parameters (black star) than FQI.

after the $K = 2$ iterations, for 8 iterations; thus, the sequence of parameters for both algorithms is composed of 8 points each, while FQI has 2. It is clear that the parameters found by FQI are considerably further to the target parameters than the ones found by both ProFQI and ProFQI_{LQR}. In particular, the latter gets the closest to the target, in line with the results in Figure 6, again evincing the accuracy of the learned PBO and the benefit of performing multiple applications of it, as expected from Theorem 2.

Experiments

We consider both ProFQI and ProDQN, comparing their performance with their regular counterparts⁴. To handle the increased complexity of the input space of the considered problems, we leverage neural network regression to model our PBO. We consider an offline setting, where we use ProFQI on car-on-hill (Ernst, Geurts, and Wehenkel 2005), and an online setting, where we use ProDQN on bicycle balancing (Randlov and Alstrøm 1998), and lunar lander (Brockman et al. 2016). We want to answer the following research question: *does PBO enable moving toward the fixed point more effectively than the empirical Bellman operator?*

⁴The code is available at <https://github.com/theovincent/PBO>

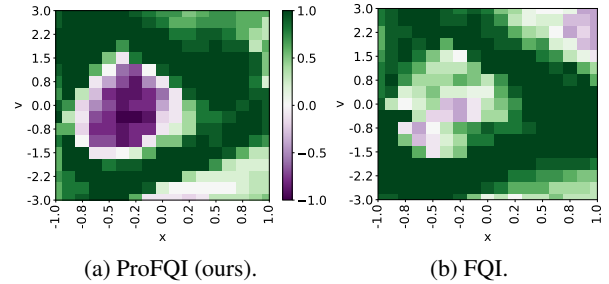


Figure 8: Policies on car-on-hill using $K = 9$ and 9 application of PBO, averaged over 20 seeds. The purple and green colors refer to the two discrete actions (move left or right). Our ProFQI approximates the optimal policy more closely.

Projected fitted Q -iteration

We initially evaluate ProFQI on the *car-on-hill* problem. As done in Ernst, Geurts, and Wehenkel (2005), we measure performance by generating roll-outs starting from different states on a grid of size 17×17 , and accounting for the fact that the dataset \mathcal{D} does not contain every starting state of the grid, by weighting the obtained performance from each starting state by the number of times it occurs in the dataset (see appendix). First, the benefit of PBO is observable in the quality of the policy computed by FQI and ProFQI (Figure 8). After only 9 training iterations, ProFQI obtains a policy that is very close to the optimal one of car-on-hill (see the well-known shape of the optimal car-on-hill policy in Figure 8a (Ernst, Geurts, and Wehenkel 2005)), while FQI is significantly more inaccurate. The consequences of this are reflected in the performance shown in Figure 9, that are obtained with FQI and ProFQI for three different values of Bellman iterations K (black dashed vertical line). Again, for FQI, K is the number of regular iterations consisting of an application of the empirical Bellman operator and the projection step; for ProFQI, K is the number of applications of PBO that are used in the training loss (Equation 3). The iterations on the x -axis in Figure 9 are the regular iterations for FQI and the applications of the trained PBO for ProFQI.

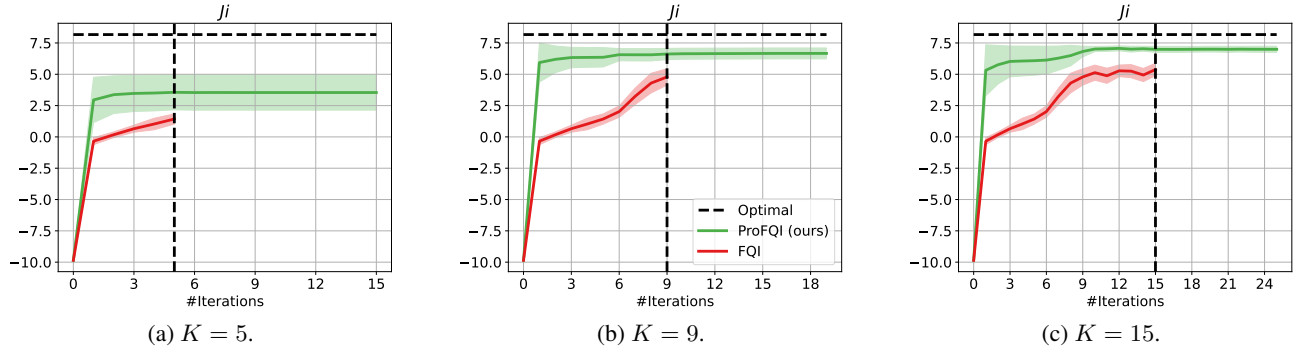


Figure 9: Discounted cumulative reward on car-on-hill. The black vertical dashed line indicates the number of iterations considered for FQI and the number of iterations K considered to train PBO. Results are averaged over 20 seeds with 95% confidence intervals. Note that ProFQI achieves higher performance than FQI and remains stable after K iterations.

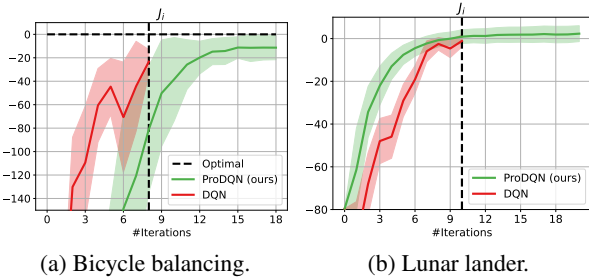


Figure 10: Discounted cumulative reward on bicycle and lunar lander. The black vertical dashed line indicates the number of target network updates performed by DQN and the number of iterations K considered to train PBO. Results are averaged over 40 seeds with 95% confidence intervals.

Thus, the iterations on the right side of the line can only be reached with ProFQI. The purpose of this analysis is to evaluate the different quality of trajectories toward the fixed point obtained by the empirical Bellman operator in FQI, and the trained PBO in ProFQI, for the same amount of transition samples. We observe that ProFQI obtains better performance than FQI consistently. This evinces that PBO learns an accurate estimate of the true Bellman operator, which allows obtaining a satisfactory action-value function faster than the standard empirical Bellman operator used by FQI. It is interesting to note that the performance of ProFQI remains stable for subsequent applications of PBO after the number of iterations used for training.

Projected deep Q -network

We also evaluate PBO in an online setting, using our ProDQN algorithm and comparing against DQN (Mnih et al. 2015). We consider a *bicycle balancing* (Randlov and Alström 1998) problem and the *lunar lander* environment (Brockman et al. 2016). We set the number of Bellman iterations $K = 8$ for bicycle balancing and $K = 10$ for the lunar lander. Similar to the offline setting, K is the number of updates of the target network for DQN, and the number of applications of PBO in the training loss (Equation 3)

for ProDQN. Due to the need to collect new samples while learning a policy, training PBO in an online setting needs a slightly different treatment than the offline case. Recalling Algorithm 1, we point out that new samples are collected after each gradient descent step, by using the action-value function obtained after K applications of the current PBO. We find this choice to work well in practice; however, we can envision multiple possibilities for effective exploration strategies based on PBO, that we postpone to future works.

Figure 10 shows the discounted cumulative reward collected by DQN and ProDQN on both bicycle balancing and lunar lander, for different numbers of iterations. For DQN, each iteration corresponds to an update of the target network, while for ProDQN it indicates an application of the trained PBO. Figure 10a shows that contrary to car-on-hill, on the bicycle balancing task ProDQN improves slower than DQN, but it keeps increasing performance after K iterations thanks to PBO. This behavior illustrates that PBO can be used after the training to move the parameters in a favorable direction (see Figure 2a (blue trajectory)). Similarly, Figure 10b shows that, on lunar lander, ProDQN keeps increasing ever so slightly, but it is also stronger than DQN overall.

Discussion and conclusion

We introduced the novel idea of an operator that directly maps parameters of action-value functions to others, as opposed to the regular Bellman operator that requires costly projections steps onto the space of action-value functions. This operator called the projected Bellman operator can generate a sequence of parameters that can progressively approach the ones of the optimal action-value function. We formulated an optimization problem and an algorithmic implementation to learn PBO in offline and online RL. One limitation of our method in its current form is that, given that the size of input and output spaces of PBO depends on the number of parameters of the action-value function, it is challenging to scale to problems that learn action-value functions with deep neural networks with millions of parameters (Mnih et al. 2015). Nevertheless, recent advances in deep learning methods for learning operators (Kovachki et al. 2021, 2023) can provide a promising future direction.

Acknowledgments

This work was funded by the German Federal Ministry of Education and Research (BMBF) (Project: 01IS22078). This work was also funded by Hessian.ai through the project 'The Third Wave of Artificial Intelligence – 3AI' by the Ministry for Science and Arts of the state of Hessen and by the grant "Einrichtung eines Labors des Deutschen Forschungszentrum für Künstliche Intelligenz (DFKI) an der Technischen Universität Darmstadt". This paper was also supported by FAIR (Future Artificial Intelligence Research) project, funded by the NextGenerationEU program within the PNRR-PE-AI scheme (M4C2, Investment 1.3, Line on Artificial Intelligence).

References

- Agarwal, A.; Kakade, S.; Krishnamurthy, A.; and Sun, W. 2020. Flambe: Structural complexity and representation learning of low rank mdps. *Advances in neural information processing systems*, 33: 20095–20107.
- Asadi, K.; and Littman, M. L. 2017. An alternative softmax operator for reinforcement learning. In *International Conference on Machine Learning*, 243–252. PMLR.
- Bas-Serrano, J.; Curi, S.; Krause, A.; and Neu, G. 2021. Logistic Q-learning. In *International Conference on Artificial Intelligence and Statistics*, 3610–3618. PMLR.
- Beck, J.; Jackson, M. T.; Vuorio, R.; and Whiteson, S. 2023. Hypernetworks in Meta-Reinforcement Learning. In *Proceedings of The 6th Conference on Robot Learning*, volume 205 of *Proceedings of Machine Learning Research*. PMLR.
- Bellemare, M. G.; Dabney, W.; and Munos, R. 2017. A distributional perspective on reinforcement learning. In *International Conference on Machine Learning*, 449–458. PMLR.
- Bellemare, M. G.; Dabney, W.; and Rowland, M. 2023. *Distributional Reinforcement Learning*. MIT Press. <http://www.distributional-rl.org>.
- Bellemare, M. G.; Ostrovski, G.; Guez, A.; Thomas, P.; and Munos, R. 2016. Increasing the action gap: New operators for reinforcement learning. In *Proceedings of the AAAI Conference on Artificial Intelligence*, volume 30.
- Bellman, R. 1966. Dynamic programming. *Science*, 153(3731): 34–37.
- Belousov, B.; and Peters, J. 2019. Entropic regularization of markov decision processes. *Entropy*, 21(7): 674.
- Bertsekas, D. 2019. *Reinforcement learning and optimal control*. Athena Scientific.
- Bertsekas, D. P. 2015. *Dynamic Programming and Optimal Control 4th Edition, Volume II*. Athena Scientific.
- Bradtke, S. 1992. Reinforcement learning applied to linear quadratic regulation. *Advances in neural information processing systems*, 5.
- Brockman, G.; Cheung, V.; Pettersson, L.; Schneider, J.; Schulman, J.; Tang, J.; and Zaremba, W. 2016. Openai gym. *arXiv preprint arXiv:1606.01540*.
- Chauhan, V. K.; Zhou, J.; Lu, P.; Molaei, S.; and Clifton, D. A. 2023. A Brief Review of Hypernetworks in Deep Learning. *arXiv preprint arXiv:2306.06955*.
- Chen, T.; and Chen, H. 1995. Universal approximation to nonlinear operators by neural networks with arbitrary activation functions and its application to dynamical systems. *IEEE Transactions on Neural Networks*, 6(4): 911–917.
- Ernst, D.; Geurts, P.; and Wehenkel, L. 2005. Tree-Based Batch Mode Reinforcement Learning. *JMLR*, 6: 503–556.
- Farahmand, A.-m. 2011. Regularization in reinforcement learning.
- Fellows, M.; Hartikainen, K.; and Whiteson, S. 2021. Bayesian Bellman Operators. *Advances in Neural Information Processing Systems*, 34: 13641–13656.
- Geist, M.; Scherrer, B.; and Pietquin, O. 2019. A theory of regularized markov decision processes. In *International Conference on Machine Learning*, 2160–2169. PMLR.
- Ha, D.; Dai, A.; and Le, Q. 2016. HyperNetworks. In *International Conference on Learning Representations*.
- Haarnoja, T.; Tang, H.; Abbeel, P.; and Levine, S. 2017. Reinforcement learning with deep energy-based policies. In *International conference on machine learning*, 1352–1361. PMLR.
- Kingma, D. P.; and Ba, J. 2015. Adam: A Method for Stochastic Optimization. In *International Conference on Learning Representations*.
- Kissas, G.; Seidman, J. H.; Guilhoto, L. F.; Preciado, V. M.; Pappas, G. J.; and Perdikaris, P. 2022. Learning operators with coupled attention. *Journal of Machine Learning Research*, 23(215): 1–63.
- Kovachki, N.; Li, Z.; Liu, B.; Azizzadenesheli, K.; Bhat-tacharya, K.; Stuart, A.; and Anandkumar, A. 2021. Neural operator: Learning maps between function spaces. *arXiv preprint arXiv:2108.08481*.
- Kovachki, N.; Li, Z.; Liu, B.; Azizzadenesheli, K.; Bhat-tacharya, K.; Stuart, A.; and Anandkumar, A. 2023. Neural operator: Learning maps between function spaces with applications to PDEs. *Journal of Machine Learning Research*, 24(89): 1–97.
- Lagoudakis, M. G.; and Parr, R. 2003. Least-squares policy iteration. *The Journal of Machine Learning Research*, 4: 1107–1149.
- Lillicrap, T. P.; Hunt, J. J.; Pritzel, A.; Heess, N.; Erez, T.; Tassa, Y.; Silver, D.; and Wierstra, D. 2015. Continuous control with deep reinforcement learning. *arXiv preprint arXiv:1509.02971*.
- Micchelli, C. A.; and Pontil, M. 2005. On learning vector-valued functions. *Neural computation*, 17(1): 177–204.
- Mnih, V.; Kavukcuoglu, K.; Silver, D.; Rusu, A. A.; Veness, J.; Bellemare, M. G.; Graves, A.; Riedmiller, M.; Fidjeland, A. K.; Ostrovski, G.; et al. 2015. Human-level control through deep reinforcement learning. *nature*, 518(7540): 529–533.
- Munos, R. 2003. Error bounds for approximate policy iteration. In *ICML*, volume 3, 560–567.

- Munos, R. 2005. Error bounds for approximate value iteration. In *Proceedings of the National Conference on Artificial Intelligence*, volume 20, 1006. Menlo Park, CA; Cambridge, MA; London; AAAI Press; MIT Press; 1999.
- Munos, R.; and Szepesvári, C. 2008. Finite-Time Bounds for Fitted Value Iteration. *Journal of Machine Learning Research*, 9(5).
- Neu, G.; Jonsson, A.; and Gómez, V. 2017. A unified view of entropy-regularized markov decision processes. *arXiv preprint arXiv:1705.07798*.
- Pang, B.; and Jiang, Z.-P. 2021. Robust reinforcement learning: A case study in linear quadratic regulation. In *Proceedings of the AAAI Conference on Artificial Intelligence*, volume 35, 9303–9311.
- Puterman, M. L. 1990. Markov decision processes. *Handbooks in operations research and management science*, 2: 331–434.
- Randlov, J.; and Alstrøm, P. 1998. Learning to Drive a Bicycle Using Reinforcement Learning and Shaping. In *Proceedings of the 15th International Conference on Machine Learning*, 463–471.
- Sarafian, E.; Keynan, S.; and Kraus, S. 2021. Recomposing the Reinforcement Learning Building Blocks with Hypernetworks. In *Proceedings of the 38th International Conference on Machine Learning*, Proceedings of Machine Learning Research, 9301–9312. PMLR.
- Sekhari, A.; Dann, C.; Mohri, M.; Mansour, Y.; and Sridharan, K. 2021. Agnostic reinforcement learning with low-rank mdps and rich observations. *Advances in Neural Information Processing Systems*, 34: 19033–19045.
- Song, Z.; Parr, R.; and Carin, L. 2019. Revisiting the softmax bellman operator: New benefits and new perspective. In *International conference on machine learning*, 5916–5925. PMLR.
- Sutton, R. S.; and Barto, A. G. 2018. *Reinforcement learning: An introduction*. MIT press.
- Tosatto, S.; D’Eramo, C.; Pajarinen, J.; Restelli, M.; and Peters, J. 2019. Exploration driven by an optimistic bellman equation. In *2019 International Joint Conference on Neural Networks (IJCNN)*, 1–8. IEEE.
- Watkins, C. J. C. H. 1989. Learning from delayed rewards.

Projected Bellman operator in low-rank Markov decision processes

Low-rank MDPs is a class of problems with two feature maps $\sigma : \mathcal{S} \times \mathcal{A} \rightarrow \mathbb{R}^d$ and $\mu : \mathcal{S} \rightarrow \mathbb{R}^d$, such that $\mathcal{P}(s'|s, a) = \langle \sigma(s, a), \mu(s') \rangle$ and $\mathcal{R}(s, a) = \langle \sigma(s, a), \theta \rangle$, for all $(s, a, s') \in \mathcal{S} \times \mathcal{A} \times \mathcal{S}$ and for $\theta \in \mathbb{R}^d$ (Agarwal et al. 2020; Sekhari et al. 2021). We assume, without loss of generality, that for all $(s, a) \in \mathcal{S} \times \mathcal{A}$, $\|\sigma(s, a)\|_1 \leq 1$ and $\max\{\|\mu(s)\|_1, \|\theta\|_1\} \leq \sqrt{d}$. The space of action-value functions is set as the space of linear functions in the parameters, i.e., $\mathcal{Q}_\Omega = \{\langle \sigma(\cdot, \cdot), \omega \rangle | \omega \in \mathbb{R}^d\}$.

Proposition 5. *In the case of continuous state and action spaces and for $\omega \in \mathbb{R}^d$, the PBO is*

$$\Lambda^*(\omega) = \theta + \gamma \int_{\mathcal{S}} \max_{a' \in \mathcal{A}} \langle \sigma(s', a') | \omega \rangle \mu(s') ds'. \quad (8)$$

The closed form is again a γ -contraction mapping assuming that the MDP has a latent variable representation.

Proofs

Closed-form of PBO for a finite MDP

Proof. We compute the optimal Bellman iteration over a table $Q \in \mathbb{R}^{N \cdot M}$

$$\begin{aligned} \Gamma^* Q(s, a) &= r(s, a) + \gamma \mathbb{E}_{s' \sim p(\cdot | s, a)} \left[\max_{a' \in \mathcal{A}} [Q(s', a')] \right] \\ &= r(s, a) + \gamma \sum_{s'} p(s' | s, a) \left[\max_{a' \in \mathcal{A}} [Q(s', a')] \right] \\ &= \left(R + \gamma P \max_{a' \in \mathcal{A}} Q(\cdot, a') \right) (s, a) \end{aligned} \quad (9)$$

where $P \in \mathbb{R}^{N \cdot M \times N}$ is the transition probability matrix of the environment. From these equations, the operator $Q \mapsto R + \gamma P \max_{a' \in \mathcal{A}} Q(\cdot, a')$, evaluated on the objective function from the definition of PBO 2, yields zero error. This means that we have found the PBO in closed form. \square

Closed-form of PBO for LQR MDP

Proof. We assume that the distribution over the samples is a discrete uniform distribution over $\mathcal{S} \times \mathcal{A}$ centered on zero in both directions. With this assumption, the optimization problem 2 is equivalent to:

$$\arg \min_{\Lambda: \Omega \rightarrow \Omega} \mathbb{E}_{\omega \sim \nu} \left[\sum_{(s, a) \in \bar{\mathcal{S}} \times \bar{\mathcal{A}}} (\Gamma^* Q_\omega(s, a) - Q_{\Lambda(\omega)}(s, a))^2 \right]$$

where $\bar{\mathcal{S}} \times \bar{\mathcal{A}}$ is the set of all possible state-action pairs that can be drawn by the distribution of samples.

Let Λ be an operator on $\Omega = \mathbb{R}^2$, $\omega = (G, I) \in \Omega$ and $(s, a) \in \bar{\mathcal{S}} \times \bar{\mathcal{A}}$. We note the first and second components of $\Lambda(\omega)$, $\Lambda_G(\omega)$ and $\Lambda_I(\omega)$, we have:

$$\Gamma^* Q_\omega(s, a) - Q_{\Lambda(\omega)}(s, a) = \begin{bmatrix} -s^2 & -2sa \end{bmatrix} \begin{bmatrix} \Lambda_G(\omega) \\ \Lambda_I(\omega) \end{bmatrix} + \Gamma^* Q_\omega(s, a) - Ma^2.$$

We note $Z(s, a) = \begin{bmatrix} -s^2 & -2sa \end{bmatrix}$, $X = [\Lambda_G(\omega) \quad \Lambda_I(\omega)]^T$ and $b(s, a) = \Gamma^* Q_\omega(s, a) - Ma^2$. By summing over the samples we get:

$$\sum_{(s, a) \in \bar{\mathcal{S}} \times \bar{\mathcal{A}}} (\Gamma^* Q_\omega(s, a) - Q_{\Lambda(\omega)}(s, a))^2 = \sum_{(s, a) \in \bar{\mathcal{S}} \times \bar{\mathcal{A}}} (Z(s, a)X + b(s, a))^2 = \|ZX + b\|_2^2$$

where $Z = \begin{bmatrix} \dots \\ Z(s, a) \\ \dots \end{bmatrix}$ and $b = [\dots \quad b(s, a) \quad \dots]^T$.

Minimizing $\|ZX + b\|_2^2$ over $X \in \Omega$ will bring us to the minimizer of the optimization problem for any parameter distribution ν . To minimize this quantity, we need to investigate the matrix

$$Z^T Z = \begin{bmatrix} \sum_s s^4 & 2 \sum_{s, a} s^3 a \\ 2 \sum_s s^3 a & 2 \sum_{s, a} s^2 a^2 \end{bmatrix} = \begin{bmatrix} \sum_s s^4 & 0 \\ 0 & \sum_{s, a} s^2 a^2 \end{bmatrix}.$$

The last equality comes from the fact that the sample distribution is symmetric along $\bar{\mathcal{S}}$ and $\bar{\mathcal{A}}$. $Z^T Z$ is positive definite so $\min_{X \in \Omega} \|ZX + b\|_2^2$ has a unique minimizer: $\Lambda^*(\omega) = -(Z^T Z)^{-1} Z^T b$.

Let us now rewrite b . The optimal Bellman iteration over Q_ω is $\Gamma^* Q_\omega(s, a) = r(s, a) + \max_{a'} Q_\omega(s', a')$. M is chosen negative so that the function $a' \mapsto Q_\omega(s', a') = G \cdot s'^2 + 2I \cdot s' a' + M \cdot a'^2$ has a unique maximizer of equation $-I/M \cdot s'$. This makes

$$\max_{a'} Q_\omega(s', a') = Q_\omega(s', -\frac{I}{M} \cdot s') = G \cdot s'^2 - 2\frac{I^2}{M} \cdot s'^2 + \frac{I^2}{M} \cdot s'^2 = (G - \frac{I^2}{M}) \cdot s'^2.$$

By inserting it into the Bellman equation, we get

$$\begin{aligned} b(s, a) &= \Gamma^* Q_\omega(s, a) - M a^2 \\ &= r(s, a) + (G - \frac{I^2}{M}) \cdot s'^2 - M a^2 \\ &= Q \cdot s^2 + 2S \cdot sa + R \cdot a^2 + (G - \frac{I^2}{M}) \cdot s'^2 - M a^2 \\ &= \left(Q + A^2(G - \frac{I^2}{M}) \right) \cdot s^2 + 2 \left(S + AB(G - \frac{I^2}{M}) \right) \cdot sa + \left(R + B^2(G - \frac{I^2}{M}) - M \right) \cdot a^2 \\ &= \begin{bmatrix} s^2 & 2sa & a^2 \end{bmatrix} \cdot \begin{bmatrix} Q + A^2(G - \frac{I^2}{M}) - G \\ S + AB(G - \frac{I^2}{M}) - I \\ R + B^2(G - \frac{I^2}{M}) - M \end{bmatrix}. \end{aligned}$$

This means that

$$\Lambda^*(\omega) = -(Z^T Z)^{-1} Z^T J \begin{bmatrix} Q + A^2(G - \frac{I^2}{M}) \\ S + AB(G - \frac{I^2}{M}) \\ R + B^2(G - \frac{I^2}{M}) - M \end{bmatrix}$$

where $J = \begin{bmatrix} s^2 & \dots & a^2 \\ 2sa & \dots & \\ \dots & \dots & \end{bmatrix}$.

From the fact that $Z^T J = \begin{bmatrix} -\sum_s s^4 & 0 & 0 \\ 0 & \sum_{s,a} s^2 a^2 & 0 \end{bmatrix}$, we have $-(Z^T Z)^{-1} Z^T J = \begin{bmatrix} 1 & 0 & 0 \\ 0 & 1 & 0 \end{bmatrix}$, thus $\Lambda^*(\omega) = \begin{bmatrix} Q + A^2(G - \frac{I^2}{M}) \\ S + AB(G - \frac{I^2}{M}) \end{bmatrix}$. □

Remarks With the assumption on the distribution of samples, the PBO can also be understood in a geometrical way. It projects the parameters along a line of direction vector $[A^2 \ AB]^T$ with an offset $[Q \ S]^T$. The iterations correspond to a non-linear transformation of the coefficient $(G - I^2/M)$ in front of the direction vector. This also means that the fixed point, i.e. the optimal parameters are also on this line.

Closed-form of PBO for a low-rank MDP

Proof. The proof considers continuous unbounded state-action spaces. For $Q_\omega \in \mathcal{Q}_\Omega$, ω the vector representing Q_ω , $\max_{a \in \mathcal{A}} Q_\omega(s, a)$ is well defined (here max might not be attained, it should be interpreted as a supremum). We have $|Q_\omega(s, a)| = |\langle \sigma(s, a) | \omega \rangle| \leq \|\sigma(s, a)\| \cdot \|\omega\| \leq \|\omega\|$, thus $\max_{a \in \mathcal{A}} Q_\omega(s, a) < \infty$. Then, we write the optimal Bellman iteration on the function Q_ω as

$$\begin{aligned} \Gamma^* Q_\omega(s, a) &= r(s, a) + \gamma \mathbb{E}_{s' \sim p(\cdot | s, a)} \left[\max_{a' \in \mathcal{A}} Q_\omega(s', a') \right] \\ &= r(s, a) + \gamma \int_{s'} \max_{a'} \langle \sigma(s', a') | \omega \rangle p(s' | s, a) ds' \\ &= \langle \sigma(s, a) | \theta \rangle + \gamma \int_{s'} \max_{a'} \langle \sigma(s', a') | \omega \rangle \langle \sigma(s, a) | \mu(s') \rangle ds' \text{ from the definition of the transition} \\ &\quad \text{probabilities.} \\ &= \langle \sigma(s, a) | \theta \rangle + \gamma \int_{s'} \max_{a'} \langle \sigma(s', a') | \omega \rangle \mu(s') ds' \text{ from the linear of the scalar product.} \end{aligned}$$

This derivation shows that the operator $\omega \mapsto \theta + \gamma \int_{s'} \max_{a'} \langle \sigma(s', a') | \omega \rangle \mu(s') ds'$ minimizes the objective function presented in the definition of PBO 2 since it yields zero error. This operator is the PBO for a low-rank MDP. □

Table 1: Summary of all parameters used in the offline experiments.

		Chain-walk	LQR	Car-on-hill	Bicycle
	horizon	$+\infty$	$+\infty$	100	50.000
	γ	0.9	1	0.95	0.99
	$\#\mathcal{D}$	400	121	5.500	70.000
	batch size on \mathcal{D}	20	121	500	1.000
FQI	#fitting steps	400	800	1.200	1.200
	#patience steps	100	100	30	7
	starting learning rate	10^{-2}	10^{-2}	10^{-3}	5×10^{-3}
	ending learning rate	10^{-5}	10^{-5}	5×10^{-7}	10^{-4}
ProFQI	$\#\mathcal{W}$	100	5	30	50
	batch size on \mathcal{W}	100	5	30	25
	#epochs	1.000	1.000	1.000	500
	#training steps	5	4	10	20
	starting learning rate	10^{-2}	10^{-2}	10^{-3}	10^{-4}
	ending learning rate	10^{-7}	10^{-5}	5×10^{-7}	10^{-7}
	initial PBO's parameters std	5×10^{-6}	5×10^{-6}	5×10^{-7}	5×10^{-7}

PBO is a γ -contraction mapping for a low-rank MDP

Proof. We now assume that the MDP has a latent variable representation. This proof was inspired by the proof of the contraction property of the Bellman Operator in Bertsekas (2015). Considering $\omega, \omega' \in \mathbb{R}^d$, we have

$$\begin{aligned}
 \|\Gamma_p^*(\omega) - \Gamma_p^*(\omega')\|_\infty &= \gamma \left\| \int_{s'} \max_{a'} \langle \sigma(s', a') | (\omega - \omega') \rangle \mu(s') ds' \right\|_\infty \\
 &= \gamma \max_{i \in \{1, \dots, d\}} \left| \int_{s'} \max_{a'} \langle \sigma(s', a') | (\omega - \omega') \rangle \mu(s')_i ds' \right| \\
 &\leq \gamma \max_{i \in \{1, \dots, d\}} \int_{s'} \max_{a'} |\langle \sigma(s', a') | (\omega - \omega') \rangle| \mu(s')_i ds' \text{ since } \mu(\cdot) \text{ is positive.} \\
 &\leq \gamma \max_{i \in \{1, \dots, d\}} \int_{s'} \max_{a'} \sum_{j \in \{1, \dots, d\}} \sigma(s', a')_j |(\omega - \omega')_j| \mu(s')_i ds' \text{ since } \sigma(\cdot, \cdot) \text{ are positive.} \\
 &\leq \gamma \max_{i \in \{1, \dots, d\}} \int_{s'} \max_{a'} \sum_{j \in \{1, \dots, d\}} \sigma(s', a')_j \mu(s')_i ds' \cdot \|\omega - \omega'\|_\infty \\
 &\leq \gamma \max_{i \in \{1, \dots, d\}} \int_{s'} \mu(s')_i ds' \cdot \|\omega - \omega'\|_\infty \text{ since } \sigma(\cdot, \cdot) \text{ are probability distributions.} \\
 &\leq \gamma \|\omega - \omega'\|_\infty \text{ since } \mu(\cdot)_i \text{ is a probability distribution for all } i.
 \end{aligned}$$

□

Details of the empirical analysis

We provide details of the experimental setting. Table 1 and 2 summarize the values of all parameters appearing in the experiments. FQI, DQN, ProFQI, and ProDQN use Adam optimizer (Kingma and Ba 2015) with a linear annealing learning rate. For FQI, the optimizer is reset at each iteration. The set of parameters \mathcal{W} is generated by sampling from a truncated normal distribution. When we use action-value functions with a neural network that has more than one hidden layer, the last one is initialized with zeros. This way, the output of a neural network parameterized by any element of \mathcal{W} is zero which makes the reward easier to learn. Among the parameters in \mathcal{W} , one is chosen to be the initial parameters used by FQI or DQN. For all the methods, the metrics have been constructed starting from the initial parameters, this is why, all the plots showing the performances share the same J_0 . As Table 1 and 2 show, the initial parameters of PBOs are always taken small enough so that applying PBO multiple times does not lead to diverging outputs.

Offline experiments

Chain-walk We consider all the possible state-action pairs 10 times as the initial dataset of samples \mathcal{D} . These 10 repetitions help the algorithms to grasp the randomness of the environment. The optimal action-value function Q^* is computed with

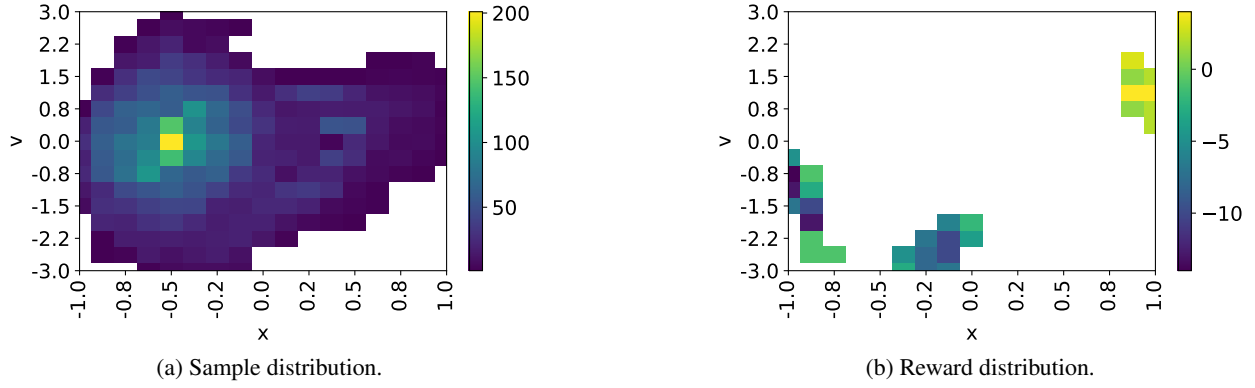


Figure 11: Composition of the dataset of samples \mathcal{D} on car-on-hill.

dynamic programming. The ℓ^2 -norm is computed by taking the norm of the vector representing the action-value function. In Figure 4, we only report the mean value, since the standard deviations over the seeds are negligible.

Linear quadratic regulator The dynamics of the system is $\mathcal{P}(s, a) = -0.46s + 0.54a$ and the reward function is $\mathcal{R}(s, a) = -0.73s^2 - 0.63sa - 0.93a^2$. M is chosen to be equal to -1.20 . The set \mathcal{D} is collected on a mesh of size 11 by 11 on the state-action space going from -4 to 4 in both directions, which means that samples belong to $[-4, 4] \times [-4, 4] \subset \mathcal{S} \times \mathcal{A}$. We choose to parameterize the value functions in a quadratic way, thus allowing us to compute the maximum in closed form. However, we assume that the algorithms do not have this knowledge since it is not the case in more general settings. For this reason, we discretize the action space in a set of 200 actions going from -8 to 8 . The architecture of the parameterized PBO trained with ProFQI is a fully connected network composed of one hidden layer having 8 neurons. Rectified linear unit (ReLU) is used as the activation function. In Figure 6, we only report the mean value, since the standard deviations over the seeds are negligible.

Car-on-hill The agent chooses between 2 actions: `left` or `right`. The state space is 2-dimensional: position in $[-1, 1]$ and velocity $[-3, 3]$. If the agent succeeds to bring the car up the hill – at a position greater than 1 and velocity in between -3 and 3 – then the reward is 1, if the agent exceeds the state space, the reward is -1 ; otherwise, the reward is 0.

As our ProFQI is an offline algorithm, we need to make sure that all the necessary exploration has been done in the dataset of samples. For that reason, we first consider a uniform sampling policy to collect episodes starting from the lowest point in the map ($[-0.5, 0]$) with a horizon of 100. This sampling process is stopped when 4.500 samples are gathered. To get more samples with positive rewards, we sample new episodes starting from a state located randomly between $[0.1, 1.3]$ and $[0.5, 0.38]$ with a uniform policy as well. In total, 5.500 samples are collected. The sample and reward distributions over the state space is shown in Figure 11. The action-value functions are parameterized with one hidden layer of 30 neurons with ReLU as activation functions. The architecture of the parameterized PBO has 4 hidden layers of 302 (2 times the number of parameters of the action-value functions) neurons each with ReLU as activation functions. To help the training, the value functions are taking actions in $\{-1, 1\}$ instead of the usual $\{0, 1\}$. Given that the policies, the reward, and the dynamics, are deterministic, we perform only one simulation to generate Figure 9.

Online experiments

Bicycle We consider the bicycle problem, as described in Randlov and Alstrøm (1998). The state space is composed of 4 dimensions: $(\omega, \dot{\omega}, \theta, \dot{\theta})$ where ω is the angle between the floor and the bike, and θ is the angle between the handlebar and the perpendicular axis to the bike. The goal is to ride a bicycle for 500 seconds (50.000 steps). The agent can apply a torque $T \in \{-2, 0, 2\}$ to the handlebar to make it rotate. The agent can also move its center of gravity in the direction $d \in \{-0.02, 0, 0.02\}$ perpendicular to the bike. As in Lagoudakis and Parr (2003), the agent chooses between applying a torque or moving its center of gravity, resulting in 5 actions instead of 9. Usually, a uniform noise in the interval $[-0.02, 0.02]$ is added to d . For the purpose of this work, we reduce the number of samples by making the magnitude of the noise 10 times smaller. A reward of -1 is given when the bike falls down, i.e., $|\omega| > 12^\circ$. We use reward shaping to have more informative samples, and we add a reward proportional to the change in ω , i.e., $10^4(|\omega_t| - |\omega_{t+1}|)$, as in Lagoudakis and Parr (2003). The dataset of samples is composed of 3.500 episodes starting from a position close to $(0, 0, 0, 0)$ and cut after 20 steps (Lagoudakis and Parr 2003). The action-value functions are parameterized with one hidden layer of 30 neurons with ReLU activations. The architecture of the parameterized PBO is composed of 3 hidden layers of 302 neurons (2 times the number of parameters of the action-value functions) each with ReLU functions as activation functions. During sampling, we only leave the algorithms 20 steps to explore before ending the episode like in the offline setting. This is done to avoid exploring regions in the state space

Table 2: Summary of all parameters used in the online experiments.

		Bicycle	Lunar Lander
horizon		50.000	1.000
γ		0.99	0.99
$\#\mathcal{D}$		10.000	1.000
max $\#\mathcal{D}$		10.000	20.000
batch size on \mathcal{D}		500	500
#steps per update		2	2
starting ϵ		1	1
ending ϵ		10^{-2}	10^{-2}
DQN	#fitting steps	6.000	6.000
	starting learning rate	10^{-4}	10^{-3}
	ending learning rate	10^{-6}	10^{-5}
ProDQN	$\#\mathcal{W}$	30	30
	batch size on \mathcal{W}	30	15
	#epochs	4.000	3.000
	#training steps	25	25
	starting learning rate	10^{-5}	10^{-5}
	ending learning rate	10^{-7}	5×10^{-7}
	initial PBO's parameters std	5×10^{-7}	5×10^{-7}

that are not useful for solving the environment. 100 simulations are done for each seed shown in Figure 10a, all of them starting from the state $(0, 0, 0, 0)$, i.e., the bicycle standing straight.

Lunar lander Lunar lander, introduced in (Brockman et al. 2016), is an environment in which the goal is to make a lunar module land at a specific location while behaving safely for the crew and the rocket. The state space is composed of 8 dimensions: the position of the rocket, the linear velocities, the angle with the horizon, the angular velocity, and two booleans for each leg being activated when they touch the ground. The action space consists of 4 actions: fire the main engine, fire the left engine, fire the right engine, and do nothing. The action-value functions are parameterized with 2 hidden layers of 30 neurons each with ReLU as activation functions. The architecture of the parameterized PBO is composed of 4 hidden layers of 2522 neurons (2 times the number of parameters of the action-value functions) each with ReLU functions as activation functions. 100 simulations are done for each seed shown in Figure 10a each of them starting from a random initial position.